G9a regulates group 2 innate lymphoid cell development by repressing the group 3 innate lymphoid cell program

Frann Antignano,[1] Mitchell Braam,[1] Michael R. Hughes,[1] Alistair L. Chenery,[1] Kyle Burrows,[1] Matthew J. Gold,[1] Menno J. Oudhoff,[1] David Rattray,[1] Timotheus Y. Halim,[3] Alissa Cait,[1] Fumio Takei,[3] Fabio M. Rossi,[1,2] Kelly M. McNagny,[1,2] and Colby Zaph[1,4]

[1]The Biomedical Research Centre and [2]Department of Medical Genetics, University of British Columbia, Vancouver, British Columbia V6T 1Z3, Canada
[3]The Terry Fox Laboratory, British Columbia Cancer Agency, Vancouver, British Columbia V5Z 1L3, Canada
[4]Infection and Immunity Program, Monash Biomedicine Discovery Institute and Department of Biochemistry and Molecular Biology, Monash University, Clayton, Victoria 3800, Australia

Innate lymphoid cells (ILCs) are emerging as important regulators of homeostatic and disease-associated immune processes. Despite recent advances in defining the molecular pathways that control development and function of ILCs, the epigenetic mechanisms that regulate ILC biology are unknown. Here, we identify a role for the lysine methyltransferase G9a in regulating ILC2 development and function. Mice with a hematopoietic cell–specific deletion of G9a (*Vav.G9a*$^{-/-}$ mice) have a severe reduction in ILC2s in peripheral sites, associated with impaired development of immature ILC2s in the bone marrow. Accordingly, *Vav.G9a*$^{-/-}$ mice are resistant to the development of allergic lung inflammation. G9a-dependent dimethylation of histone 3 lysine 9 (H3K9me2) is a repressive histone mark that is associated with gene silencing. Genome-wide expression analysis demonstrated that the absence of G9a led to increased expression of ILC3-associated genes in developing ILC2 populations. Further, we found high levels of G9a-dependent H3K9me2 at ILC3-specific genetic loci, demonstrating that G9a-mediated repression of ILC3-associated genes is critical for the optimal development of ILC2s. Together, these results provide the first identification of an epigenetic regulatory mechanism in ILC development and function.

Innate lymphoid cells (ILCs) reside primarily at barrier surfaces where they play key roles in maintaining mucosal homeostasis and protecting against infection. Similar to $CD4^+$ Th cells, ILCs can be grouped according to cytokine production and transcription factor expression. For example, group 2 ILCs (ILC2s) express the transcription factor GATA3 and produce the cytokines IL-5 and IL-13 in response to the epithelial cell–derived cytokines IL-25, IL-33, and thymic stromal lymphopoietin, whereas ILC3s express RORγt and produce high levels of IL-17A, IL-17F, and IL-22 after stimulation with IL-23.

In adult mice, both ILC2s and ILC3s can develop from the common lymphoid progenitor (CLP) in the BM (Possot et al., 2011; Hoyler et al., 2012), which is followed developmentally by a common helper-like ILC progenitor (ChILP) that expresses the transcription factor Id2 and the integrin α4β7 and responds to IL-7 (Moro et al., 2010; Cherrier et al., 2012; Klose et al., 2014). However, the mechanisms controlling the lineage choice between ILC2s and ILC3s are unclear. ILC2 development is regulated by expression of several factors including TCF-1, Notch (Yang et al., 2013), RORα (Halim et al., 2012b; Wong et al., 2012), GATA3 (Hoyler et al., 2012), promyelocytic leukemia zinc finger protein (PLZF; Constantinides et al., 2014), and Gfi1 (Spooner et al., 2013). ILC3 development is mediated primarily through expression of the nuclear hormone receptor RORγt (Kurebayashi et al., 2000; Sun et al., 2000; Eberl et al., 2004; Sanos et al., 2009; Satoh-Takayama et al., 2010), although a role for GATA3 in ILC3 development has also been shown (Serafini et al., 2014; Yagi et al., 2014). Furthermore, recent studies demonstrated that Gfi1 (Spooner et al., 2013) and Bcl11b (Califano et al., 2015) are required to repress a subset of ILC3-specific genes, including *Ahr*, *Rorc*, *Il17a*, and *Il17f*. Thus, ILC2 and ILC3 developmental programs are intimately linked, and repression of one subset may be required to allow the development of the other.

G9a (Ehmt2 and Kmt1c) is a lysine methyltransferase that is responsible for the dimethylation of lysine 9 of histone H3 (H3K9me2; Tachibana et al., 2002). Studies in embryonic stem cells have demonstrated that G9a-dependent H3K9me2 is required for gene silencing and is acquired at lineage-promiscuous genes as cells differentiate (Wen et al., 2009; Chen et al., 2012). However, we recently demonstrated that G9a is dispensable for lineage-promiscuous gene silencing in Th cells and that G9a, but not its methyltransferase

Correspondence to Colby Zaph: colby.zaph@monash.edu; or Frann Antignano: frann@brc.ubc.ca

Abbreviations used: BAL, bronchoalveolar lavage; ChILP, common helper-like ILC progenitor; ChIP, chromatin immunoprecipitation; CLP, common lymphoid progenitor; HDM, house dust mite; iILC2, immature ILC2; ILC, innate lymphoid cell; mLN, mesenteric LN; PAS, periodic acid-Schiff; RT-PCR, real-time PCR; VAT, visceral adipose tissue.

The Rockefeller University Press $30.00
J. Exp. Med. 2016 Vol. 213 No. 7 1153–1162
www.jem.org/cgi/doi/10.1084/jem.20151646

activity, is required for promoting Th2 cell differentiation (Lehnertz et al., 2010; Antignano et al., 2014). Based on the similarities between Th cells and ILCs, we sought to define the role of G9a in ILCs.

Here, we show that G9a is a cell-intrinsic regulator of ILC2 development, differentiation, and function. Loss of G9a or inhibition of its methyltransferase activity resulted in a loss of repression of the ILC3 lineage, expression of ILC3-associated genes, and increased numbers of ILC3s in the periphery. In WT immature ILC2s (iILC2s), repressive H3K9me2 marks were found at high levels at ILC3-associated genes but at low levels at the promoters of the actively transcribed ILC2-specific genes *Il5* and *Il13*. Thus, the results presented here provide the first evidence of an epigenetic regulatory pathway in ILC2s and identifies G9a-dependent H3K9me2 as a critical repressive mechanism to regulate ILC2 development.

RESULTS AND DISCUSSION

G9a regulates ILC2 development

To study the role of G9a in ILC development, we generated mice with a hematopoietic cell–specific deletion of G9a (termed *Vav.G9a*$^{-/-}$ mice) by crossing mice with a floxed allele of *G9a* (*G9a*$^{fl/fl}$ mice; Lehnertz et al., 2010) with mice expressing Cre recombinase under the control of the *Vav* promoter. We analyzed the generation of iILC2s in the BM during steady-state hematopoiesis by flow cytometric analysis of Lin$^-$ c-kit^{low} Sca-1^{high} CD25$^+$ CD127$^+$ cells (Halim et al., 2012b; Hoyler et al., 2012). Despite having a significant expansion of Lin$^-$ c-kit^{low} Sca-1^{high} cells, we found a significant reduction in the frequency of iILC2s in the BM of *Vav.G9a*$^{-/-}$ mice compared with control *G9a*$^{fl/fl}$ mice (Fig. 1 A). During development from a CLP to iILC2, receptors for the cytokines IL-33 (ST2 and *Il1rl1*) and IL-25 (IL-17RB) are up-regulated (Halim et al., 2012b; Wong et al., 2012; Constantinides et al., 2014). We found that iILC2s from *G9a*$^{fl/fl}$ mice expressed high levels of ST2, whereas only ∼50% of iILC2s from *Vav.G9a*$^{-/-}$ mice expressed ST2 (Fig. 1 A), resulting in a 75% reduction in the number of Lin$^-$ c-kit^{low} Sca-1^{high} CD25$^+$ CD127$^+$ ST2$^+$ iILC2s in the absence of G9a (Fig. 1 B). In contrast to ST2, IL-17RB was expressed at equivalent levels by iILC2s from both *G9a*$^{fl/fl}$ and *Vav.G9a*$^{-/-}$ mice (Fig. 1 C). In addition, BM iILC2s have been found to express the transcription factor GATA3 (Hoyler et al., 2012). We found that nearly all *G9a*$^{fl/fl}$ Lin$^-$ c-kit^{low} Sca-1^{high} CD25$^+$ CD127$^+$ cells expressed GATA3, but in the absence of G9a, only the ST2$^+$ cells expressed GATA3 (Fig. 1 D). Systemic administration of IL-33 results in an expansion of ILC2s in the BM (Spooner et al., 2013). In response to IL-33, control *G9a*$^{fl/fl}$ mice showed a significant increase in the number of BM iILC2s, whereas treatment with IL-33 failed to induce comparable ILC2 development in the BM of *Vav.G9a*$^{-/-}$ mice (Fig. 1 E). Thus, G9a plays an important role in ILC2 development, potentially through the regulation of IL-33 responsiveness.

To determine whether G9a functioned in a cell-autonomous manner in regulating the development of ILC2s, we reconstituted lethally irradiated CD45.1$^+$ mice with mixed BM harvested from congenic WT (CD45.1/2$^+$) mice and CD45.2$^+$ *G9a*$^{fl/fl}$ or *Vav.G9a*$^{-/-}$ mice. Although a 50:50 mix of donor BM (WT/*G9a*$^{fl/fl}$) yielded chimeric recipient mice with an ∼50:50 ratio of donor-derived hematopoietic cells, a 20:80 ratio of donor BM (WT/*Vav.G9a*$^{-/-}$) was required to achieve comparable chimerism. Furthermore, despite transplanting four times as many BM cells from *Vav.G9a*$^{-/-}$ CD45.2$^+$ mice, the *G9a*-deficient BM failed to give rise to iILC2s (Fig. 1, F and G). As *Vav.Cre* deletes early during hematopoiesis, it remains to be determined at what stage during ILC development G9a becomes important. We found that the absence of G9a does not affect the number of BM CLPs, but ChILPs and $\alpha_4\beta_7^+$ lymphoid progenitors (αLPs) were both reduced in the absence of G9a (Fig. 1 H), suggesting that G9a is important for differentiation of ILC progenitors downstream of the CLP.

G9a regulates peripheral ILC2 responses

ILC2s have been shown to be an important innate source of type 2 cytokines in the mesenteric LNs (mLNs; Neill et al., 2010), the lungs (Halim et al., 2012a), and visceral adipose tissue (VAT; Moro et al., 2010). We found that *Vav.G9a*$^{-/-}$ mice have significantly fewer ILC2s in the mLNs, lungs, and VAT (Fig. 2, A and B) compared with *G9a*$^{fl/fl}$ mice, but unlike in the BM, those that were present in the periphery expressed comparable levels of ST2 (Fig. 2 C). Thus, it is likely that the small number of ST2$^+$ iILC2s in the BM of *Vav.G9a*$^{-/-}$ mice that were able to express GATA3 (Fig. 1 D) populated the peripheral tissues, albeit at significantly lower levels than *G9a*$^{fl/fl}$ mice.

G9a regulates ILC2 function during lung inflammation

Treatment of mice intranasally with the protease papain has been shown to induce ILC2-dependent IL-5 and IL-13 production, eosinophilia, and lung inflammation (Oboki et al., 2010; Halim et al., 2012a). After a short course of papain treatment, *Vav.G9a*$^{-/-}$ mice had reduced expression of *Il5* and *Il13* in the lungs and significantly reduced influx of eosinophils into the bronchoalveolar lavage (BAL) fluid compared with control *G9a*$^{fl/fl}$ mice, despite equivalent eosinophil numbers in the steady state (Fig. 3 A). In addition, after papain treatment of *Vav.G9a*$^{-/-}$ mice on a *Rag1*$^{-/-}$ background (*Rag.Vav.G9a*$^{-/-}$), we observed significantly reduced eosinophilic influx into the BAL fluid compared with *Rag.G9a*$^{fl/fl}$ mice (Fig. 3 B). After a longer course of papain administration (Spooner et al., 2013; Halim et al., 2014), we found that *Vav.G9a*$^{-/-}$ mice had significantly fewer ILC2s and eosinophils in the lungs than control *G9a*$^{fl/fl}$ mice (Fig. 3 C). Thus, G9a controls ILC2 function during papain-induced lung inflammation.

We have recently shown that ILC2s facilitate the local development of a Th2 cell response in the house dust mite

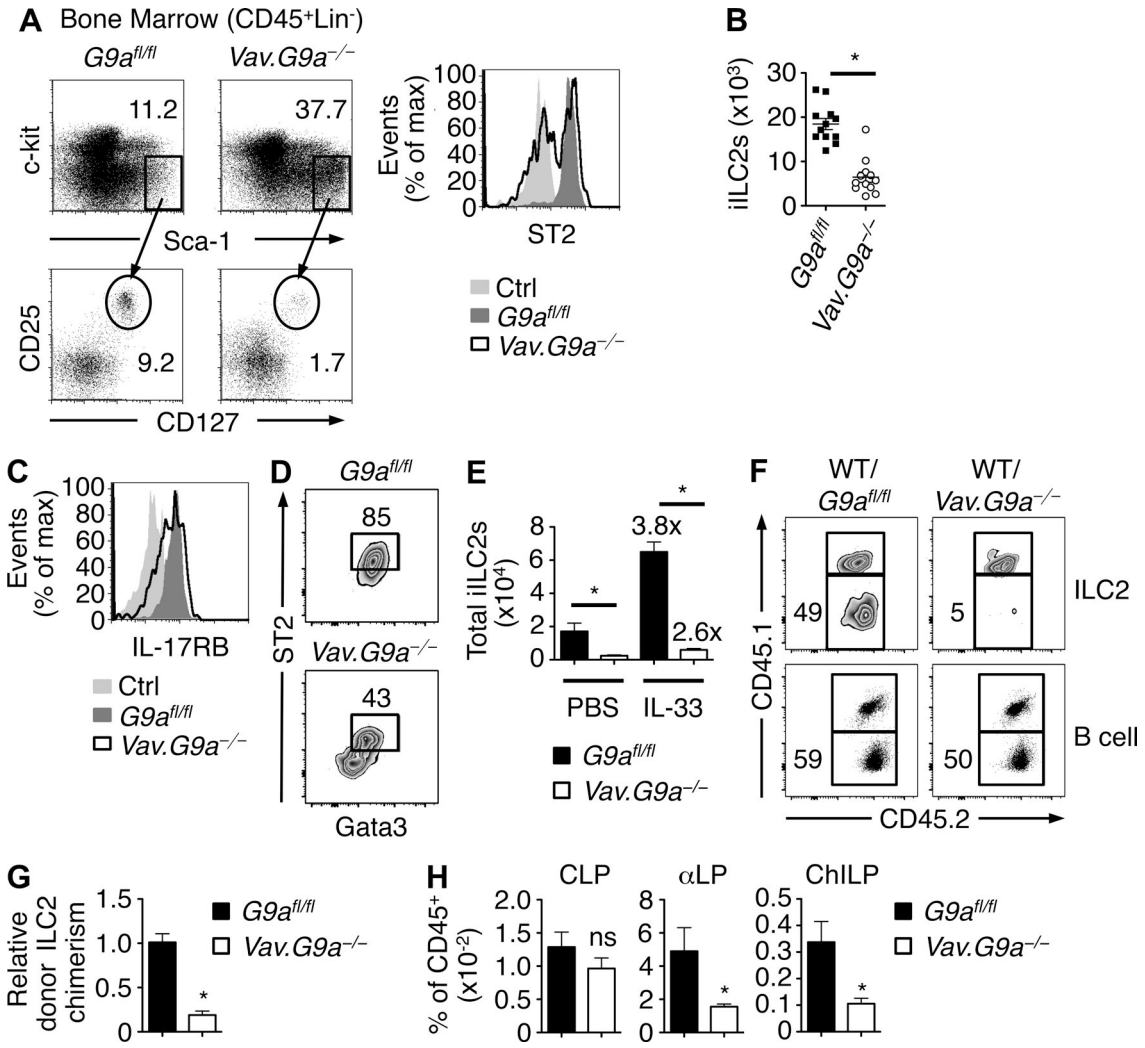

Figure 1. **G9a regulates the development of iILC2s.** (A) Frequencies of iILC2s in *G9a*$^{fl/fl}$ and *Vav.G9a*$^{-/-}$ mice. The numbers show percentages of gated cells ($n > 12$). (B) Absolute numbers of iILC2s in BM ($n = 12$ mice per genotype). (C) IL-17RB expression on BM iILC2s from *Vav.G9a*$^{-/-}$ mice (black line) and control *G9a*$^{fl/fl}$ mice (dark gray; $n = 5$). The light gray shaded area represents the negative control (Ctrl). (D) ST2 and GATA3 expression in BM iILC2s from *G9a*$^{fl/fl}$ or *Vav.G9a*$^{-/-}$ mice. Data are representative of two independent experiments ($n = 2$–3 per experiment). (E) Absolute numbers of BM ILC2s in *Vav.G9a*$^{-/-}$ mice and control *G9a*$^{fl/fl}$ mice after treatment with PBS or IL-33. Data are from three independent experiments ($n = 5$ for PBS and $n = 11$ for IL-33). (F) Reconstitution of mixed BM chimeras of *Vav.G9a*$^{-/-}$ BM and control *G9a*$^{fl/fl}$ BM competed with CD45.1/2 BM and together injected into lethally irradiated CD45.1 mice was examined 8–12 wk after transplant. (G) Relative iILC2 chimerism normalized to splenic B cells. Data are from two of three independent experiments ($n = 4$–5 mice per experiment). (H) Frequencies of CLPs (CD45$^+$ Lin$^-$ CD127$^+$ Flt3$^+$ $\alpha_4\beta_7^-$), $\alpha_4\beta_7^+$ lymphoid progenitors (αLP; CD45$^+$ Lin$^-$ CD127$^+$ Flt3$^-$ $\alpha_4\beta_7^+$), and ChILPs (CD45$^+$ Lin$^-$ CD127$^+$ Flt3$^-$ $\alpha_4\beta_7^+$ CD25$^-$ c-Kit$^+$). Data are from three independent experiments ($n = 7$). ns, not significant. *, $P < 0.05$; Student's *t* test. Errors bars indicate SEM.

(HDM) model of allergic lung inflammation (Gold et al., 2014). Similar to results with papain, we found that numbers of ILC2s in the lungs as well as numbers of eosinophils in the BAL fluid of *Vav.G9a*$^{-/-}$ mice were significantly reduced compared with *G9a*$^{fl/fl}$ mice (Fig. 3 D). Expression of *Il5* and *Il13* was also reduced in the lungs of *Vav.G9a*$^{-/-}$ mice (Fig. 3 E). Consistent with these results, we observed significantly reduced goblet cell hyperplasia in the lungs of HDM-treated *Vav.G9a*$^{-/-}$ mice (Fig. 3, F and G). As numbers of ILC2s are reduced in the absence of G9a, we also wanted to determine whether the remaining ILC2s are functionally competent. To test this, we sorted equivalent numbers of mature ILC2s from the lungs of naive *G9a*$^{fl/fl}$ and *Vav.G9a*$^{-/-}$ mice and stimulated them with IL-33 and thymic stromal lymphopoietin (Halim et al., 2012a). We found a significant reduction in IL-5 and IL-13 production (Fig. 3 H), highlighting a role for G9a in promoting ILC2-dependent gene expression in mature ILC2s. Thus, these results demonstrate that G9a is a critical regulator of ILC2-dependent lung inflammation.

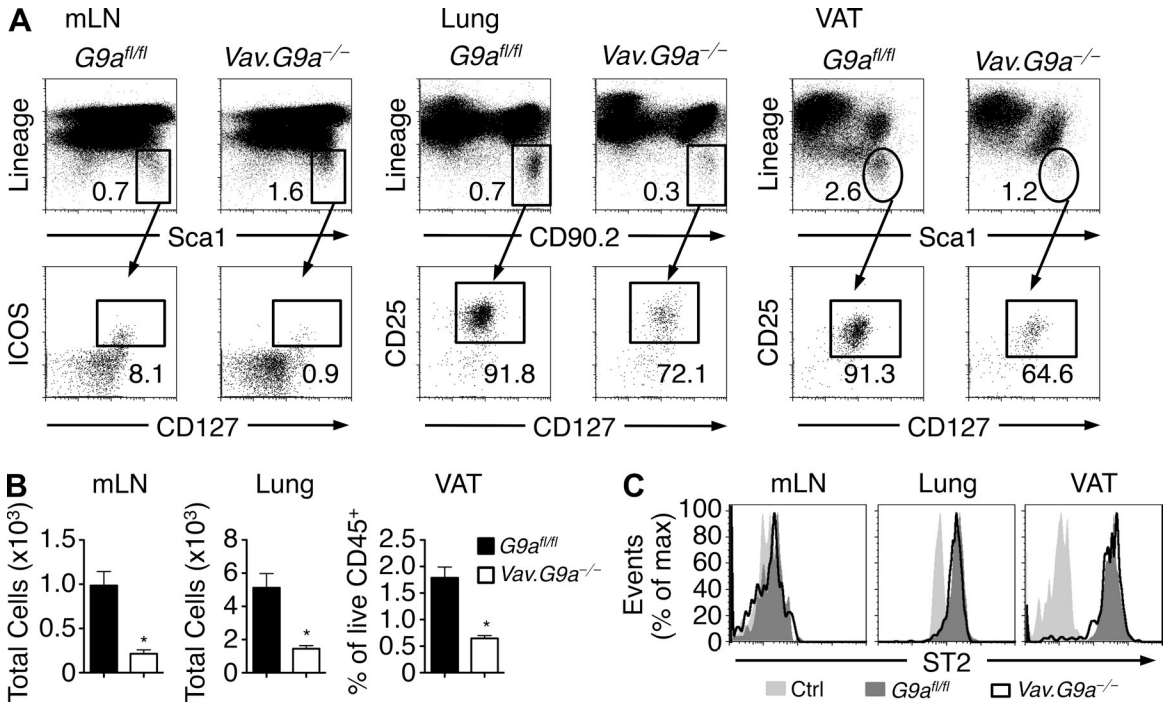

Figure 2. **G9a-deficient mice lack tissue ILC2s.** (A) Frequencies of ILC2s in the mLN, lung, and VAT of *G9a*$^{fl/fl}$ and *Vav.G9a*$^{-/-}$ mice. ICOS, inducible T cell co-stimulator. (B) Quantification of total ILC2s (mLN, $n = 9–10$; and lung, $n = 6$) or frequency of live CD45$^+$ (VAT, $n = 4$). (C) Representative expression of ST2 in mature ILC2s from *G9a*$^{fl/fl}$ (dark gray) and *Vav.G9a*$^{-/-}$ mice (black line). Light gray represents the negative control (Ctrl). *, $P < 0.05$; Student's *t* test. Errors bars indicate SEM.

G9a regulates the ILC2-specific effector state by repressing ILC3-specific genes

We next used genome-wide expression analysis to identify the molecular signature of *G9a*-deficient ILC2s. We sorted CD45$^+$ Lin$^-$ c-kit^{low} Sca-1^{high} CD25$^+$ ST2$^+$ iILC2s from the BM of *G9a*$^{fl/fl}$ or *Vav.G9a*$^{-/-}$ mice and expanded them in vitro for 10 d in the presence of IL-2, IL-7, and IL-25. Consistent with our in vivo findings, in vitro expanded iILC2s from *Vav.G9a*$^{-/-}$ mice expressed lower levels of well characterized ILC2-specific genes including *Il1rl1*, *Crlf2*, *Il5*, *Il13*, *Areg* (amphiregulin), *Gata3*, and *Icos* (inducible T cell co-stimulator; Fig. 4 A). Over 70% of the core ILC2 genes (Robinette et al., 2015) show reduced expression in the absence of G9a (Fig. 4 B and Table S1), suggesting that G9a is a central control point in ILC2 development. Strikingly, we found that expression of ILC3-associated genes such as *Il1r1*, *Il23r*, *Rorc*, *Il17f*, *Il22*, and *Lta* was significantly higher in ILC2s from *Vav.G9a*$^{-/-}$ mice (Fig. 4 A). Indeed, >80% of the core ILC3 genes were increased in *G9a*-deficient ILC2s (Fig. 4 B). These results demonstrate that G9a serves an important function in promoting ILC2 development while inhibiting the ILC3-associated gene expression program.

In the absence of G9a, we observed a reduction in the frequency of ILC2s producing IL-5, and the production of IL-17F was only seen in cultures of G9a-deficient ILC2s (Fig. 4 C). Critically, IL-17F–producing cells were distinct from IL-5–producing cells, suggesting that G9a specifically represses ILC3 differentiation in developing iILC2s. We found that ∼7.5% of the ST2$^-$ fraction of the Lin$^-$ c-kit^{low} Sca-1^{high} CD25$^+$ cells from the BM of *Vav.G9a*$^{-/-}$ mice were RORγt$^+$, compared with <1% in the ST2$^+$ fraction of either *Vav.G9a*$^{-/-}$ or *G9a*$^{fl/fl}$ cells (Fig. 4 D), suggesting that loss of G9a in iILC2s leads to ectopic expression of ILC3-associated genes. Next, we examined whether transfer of iILC2s from *Vav.G9a*$^{-/-}$ mice into NOD-Scid *Il2rg*$^{-/-}$ (NSG) mice (Halim et al., 2012b) would result in the development of both mature ILC2s and mature ILC3s. We transferred 5,000 iILC2s (CD45$^+$ Lin$^-$ c-kit^{low} Sca-1^{high} CD25$^+$CD127$^+$) isolated from the BM of *G9a*$^{fl/fl}$ or *Vav.G9a*$^{-/-}$ mice into NSG mice and analyzed the small intestine and lungs 3–4 wk later. We found that all of the ILCs in the small intestine of NSG mice that received iILC2s from *G9a*$^{fl/fl}$ mice were mature ILC2s based on KLRG1 (killer cell lectin-like receptor subfamily G member 1) expression (Hoyler et al., 2012), whereas G9a-deficient iILC2s gave rise primarily to ILC3s based on RORγt expression (Fig. 4 E). We found a similar result in the lungs with *G9a*$^{fl/fl}$ iILC2s generating mature ILC2s, and G9a-deficient iILC2s were able to generate both mature ILC2s and ILC3s despite the fact that ILC3s are normally restricted from the lungs in the steady state (Fig. 4 E; Halim et al., 2012b). Therefore, G9a is required to repress the ILC3 potential of iILC2s.

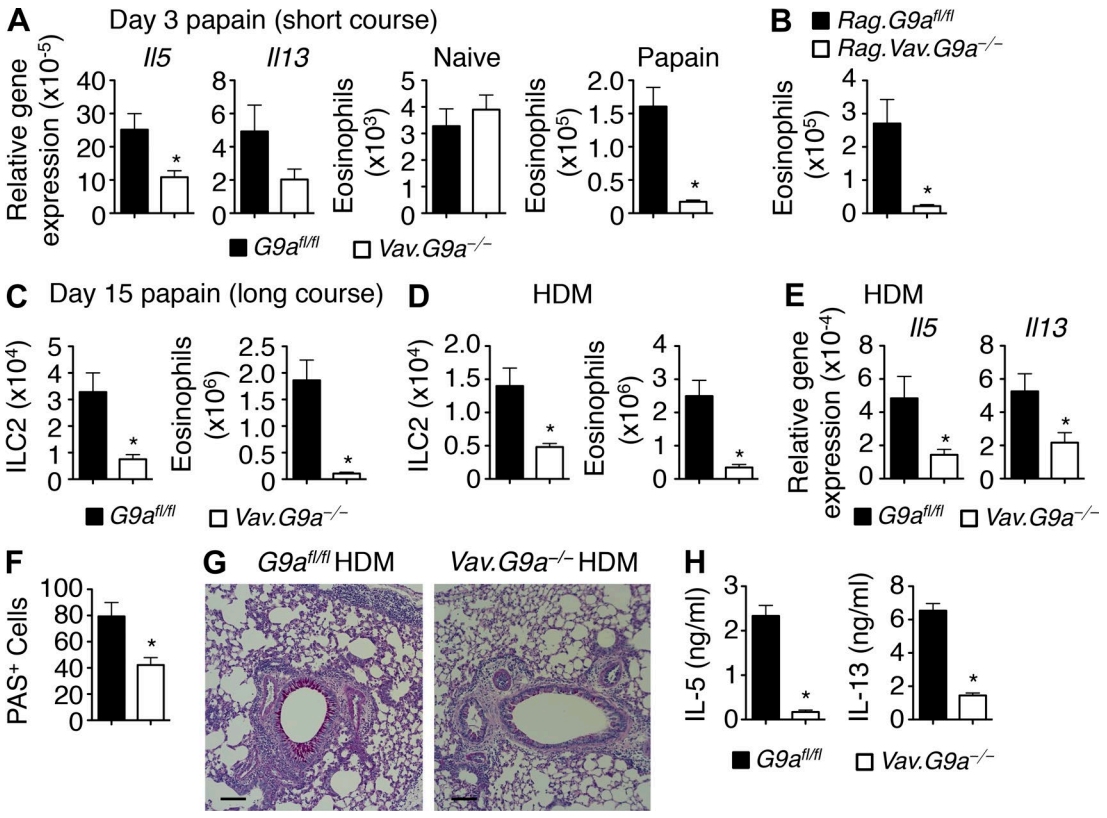

Figure 3. **G9a-deficient mice are protected from papain and HDM-induced lung eosinophilia.** (A) *G9a*$^{fl/fl}$ and *Vav.G9a*$^{-/-}$ mice were intranasally challenged with a short course of papain. Mice were sacrificed 24 h after the last challenge. Expression of *Il5* and *Il13* in lungs was measured by quantitative RT-PCR. Quantification of eosinophils in the BAL of naive and papain-treated mice as determined by flow cytometry is shown. Data are from three independent experiments (n = 4–7 per experiment). (B) *Rag.G9a*$^{fl/fl}$ mice and *Rag.Vav.G9a*$^{-/-}$ mice were intranasally challenged with a short course of papain. Mice were sacrificed 24 h after the last challenge. Quantification of eosinophils in the BAL was determined by flow cytometry. Data are from two independent experiments (n = 4–7 per experiment). (C) Number of ILC2s in the lungs and eosinophils in the BAL were quantified after a long course of papain. Data are from two independent experiments (n = 3–7 per experiment). (D) Numbers of ILC2s in the lung and eosinophils in the BAL were quantified after administration of HDM antigen. (E) Expression of *Il5* and *Il13* in lungs was measured by quantitative RT-PCR. (F) The number of PAS$^+$ goblet cells per field in the large airways was enumerated. (G) PAS-stained lung sections. Bars, 100 µm. (H) IL-5 and IL-13 production by equal numbers of ILC2s purified from the lungs of *G9a*$^{fl/fl}$ or *Vav.G9a*$^{-/-}$ mice. The data shown are representative of four independent experiments (n = 3–6 per experiment). (D–G) Data are from three independent experiments with n = 4–9 per experiment. *, $P < 0.05$; Student's t test. Errors bars indicate SEM.

Consistent with our results, we found a threefold increase in the frequency of ILC3s in the Peyer's patches and small intestinal lamina propria of *Vav.G9a*$^{-/-}$ mice compared with *G9a*$^{fl/fl}$ controls (Fig. 4 F), demonstrating that G9a is required to limit the differentiation of ILC3s. However, it remained to be determined whether G9a is also required to repress the ILC3 gene program in terminally differentiated ILC2s. To test this directly, we treated *G9a*$^{fl/fl}$ and *Vav.G9a*$^{-/-}$ mice with a short course of papain and isolated cells from the lungs, stimulated them ex vivo, and looked at cytokine production. We found increased production of IL-17A after stimulation of mature lung ILC2s, suggesting that repression of ILC3 cytokines in mature ILC2s requires G9a. We also saw a significant reduction in IL-13 production (Fig. 4 G), highlighting a role for G9a in promoting ILC2-dependent gene expression in mature ILC2s. It is noteworthy that unlike Gfi1-deficient mice, IL-17A–producing cells were mainly distinct from IL-13–producing cells, with only a few cells coexpressing the two cytokines. Thus, G9a is required to silence the ILC3 program in developing iILC2s as well as mature ILC2s.

G9a-dependent H3K9me2 is enriched at the promoters of ILC3 genes in ILC2s

Next, we cultured sorted iILC2s from the BM of WT mice in the presence of IL-2, IL-7, IL-25, and the G9a-specific methyltransferase inhibitor UNC0638 (Vedadi et al., 2011). Similar to the phenotype of iILC2s derived from *Vav.G9a*$^{-/-}$ mice, inhibition of G9a methyltransferase activity in WT iILC2s resulted in reduced expression of *Il5* and *Il13*, with a concomitant increase in expression of the ILC3-associated genes *Rorc* and *Il17f* (Fig. 5 A). Based on these results, we examined the levels of H3K9me2 at various ILC2- and ILC3-re-

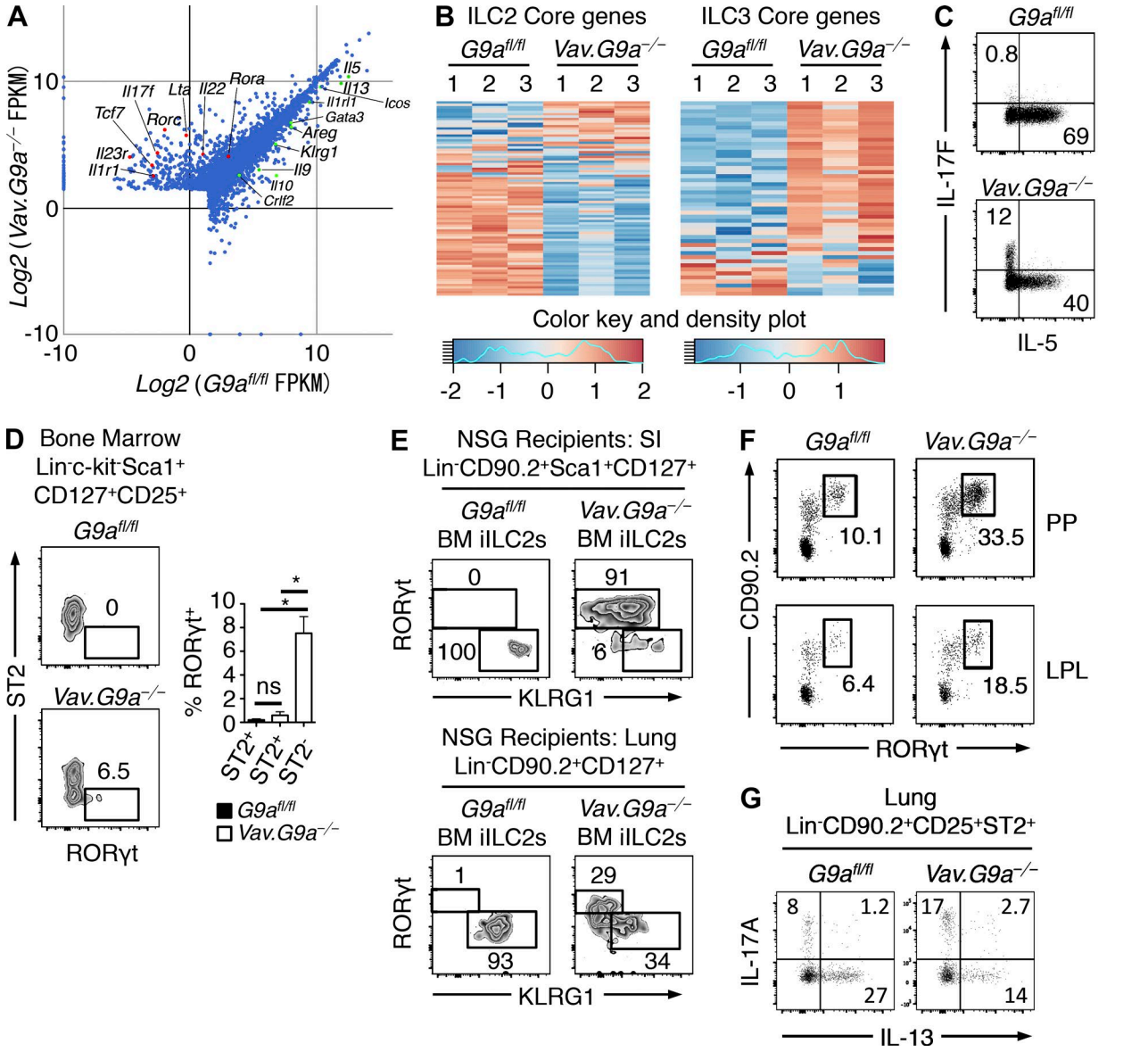

Figure 4. **Loss of G9a in iILC2s results in an ILC3 phenotype.** (A) RNA-Seq analysis of IL-2–, IL-7–, and IL-25–expanded BM iILC2s showing differential of expression down-regulated genes (green) and up-regulated (red) in *Vav.G9a*$^{-/-}$ cells relative to control *G9a*$^{fl/fl}$ cells. Data are from $n = 3$ mice per genotype. FPKM, fragments per kilobase of transcript per million mapped reads. (B) Heat maps of the expression of ILC2 and ILC3 core genes obtained from the RNA-Seq data in A. (C) Intracellular expression of IL-17F and IL-5 from sorted and expanded BM iILC2s treated with PMA, ionomycin, and brefeldin A for 4 h. The numbers in the quadrants indicate percentage of cells in each. Data are representative of three independent experiments. (D) ST2 and RORγt expression in BM iILC2s from *G9a*$^{fl/fl}$ or *Vav.G9a*$^{-/-}$ mice. Data are representative of two independent experiments ($n = 2$–3 per experiment). ns, not significant. *, $P < 0.05$; Student's *t* test. Errors bars indicate SEM. (E) RORγt and KLRG1 expression on CD45.2$^+$ Lin$^-$ CD90.2$^+$ Sca1$^+$ CD127$^+$ cells isolated from of the small intestine (SI) and CD45.2$^+$ Lin$^-$ CD90.2$^+$ CD127$^+$ cells isolated from the lungs of NSG mice 3–4 wk after transfer of iILC2s from *G9a*$^{fl/fl}$ or *Vav.G9a*$^{-/-}$ mice. Data are representative of two independent experiments ($n = 1$–2 per experiment). (F) Frequencies of ILC3s (live CD45$^+$ Lin$^-$ CD90.2$^+$ RORγt$^+$) in Peyer's patches (PP) and small intestinal lamina propria of *G9a*$^{fl/fl}$ or *Vav.G9a*$^{-/-}$ mice. Data are representative of $n = 4$ mice per genotype. LPL, lamina propria lymphocyte. (G) Intracellular expression of IL-17A and IL-13 from *G9a*$^{fl/fl}$- or *Vav.G9a*$^{-/-}$-gated lung ILC2s. After a short course of papain, cells were treated with cell stimulation cocktail (plus protein transport inhibitors) for 4 h. The numbers in the quadrants indicate the percentage of cells in each. The data are concatenated plots from three individual mice and are representative of two independent experiments ($n = 3$ per experiment).

lated gene loci in cytokine-expanded iILC2s from *G9a*$^{fl/fl}$ and *Vav.G9a*$^{-/-}$ mice by chromatin immunoprecipitation (ChIP). We detected high levels of G9a-dependent H3K9me2 at the *Il17f* and *Rorc* promoters in iILC2s from *G9a*$^{fl/fl}$ mice, consistent with its lack of expression in ILC2s (Fig. 5 B). Despite reduced *Il13* and *Il5* expression in *G9a*-deficient ILC2s, we

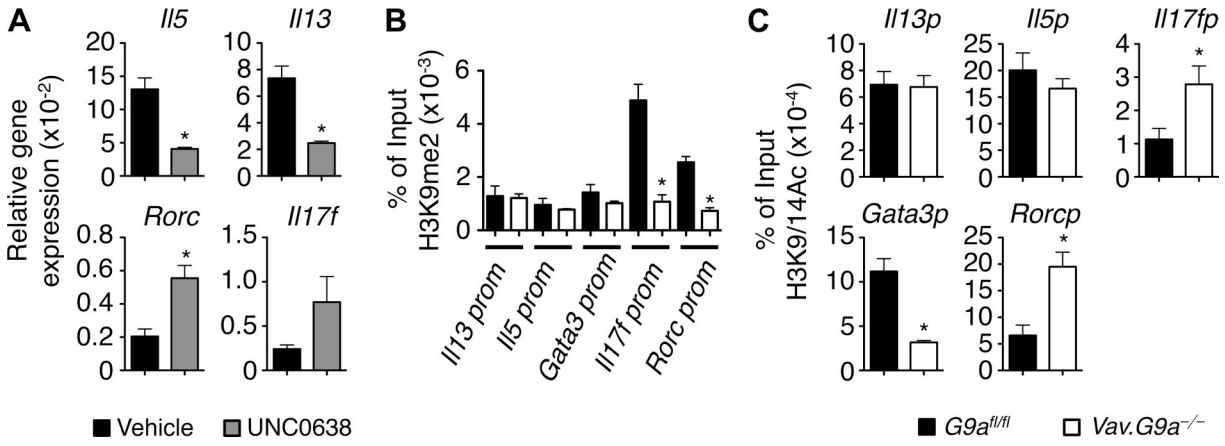

Figure 5. **Altered effector state is G9a methyltransferase dependent.** (A) Quantitative RT-PCR analysis of the indicated genes from sorted BM iILC2s expanded for 10 d in IL-2, IL-7, and IL-25 in the presence or absence of UNC0638. Data are from two independent experiments (n = 6–7 per treatment). (B and C) BM iILC2s expanded for 14 d in IL-2, IL-7, and IL-25 and processed for ChIP analysis using antibodies specific for H3K9me2 (B) or H3K9/14Ac (C). Quantitative PCR was performed using primers for the promoters of the specified genes. Data shown are from three to five independent experiments performed in triplicate. *, $P < 0.05$; Student's t test. Errors bars indicate SEM.

found no difference in the levels of acetylated H3K9/14 (H3K9/14Ac), an activating histone modification, at the promoters for *Il13 or Il5* (Fig. 5 C); however, we did see reduced levels at the *Gata3* promoter (Fig. 5 C), suggesting that ILC2 lineage identity is reduced in the absence of G9a. In addition, consistent with the heightened production of IL-17F by G9a-deficient iILC2s, we found increased levels of H3K9/14Ac at the *Il17f* and *Rorc* promoters (Fig. 5 C). Despite the importance of G9a-mediated H3K9me2 in the repression of ILC3 genes in ILC2s, we did not see any differences in G9a expression levels in ILC2s versus ILC3s in WT mice (unpublished data). Thus, G9a-dependent H3K9me2 is associated with repression of the *Il17f* and *Rorc* loci in ILC2s, and the absence of G9a leads to increased epigenetic activation and expression of ILC3-associated genes.

These results define the first epigenetic regulatory mechanism that controls ILC development, differentiation, and function. G9a-dependent H3K9me2 is required for silencing of ILC3-associated genes in iILC2s and suppression of ILC3 development. Further, G9a is required to promote expression of ILC2-associated genes in mature ILC2s. Interestingly, a recent study demonstrated that ILCs from mice with a deletion in the transcription factor Gfi1 display decreased frequencies of ILC2s and dysregulated expression of ILC3-associated genes (Spooner et al., 2013), a phenotype similar to G9a-deficient ILC2s. As Gfi1 has been shown to directly interact with G9a (Duan et al., 2005), our results suggest that G9a–Gfi1 interactions may be critically important in the epigenetic regulation of ILC development. Collectively, the results presented here identify an additional level of regulation of ILC2/ILC3 development and suggest that modulation of G9a activity may provide a novel therapeutic strategy to treat diseases associated with dysregulated ILC responses.

MATERIALS AND METHODS

Mice. *Vav.G9a*$^{-/-}$ mice and control *G9a*$^{fl/fl}$ on a C57BL/6 background, which have been previously described (Lehnertz et al., 2010), B6.SJL-*Ptprc*^{a}*Pepc*^{b}/BoyJ (CD45.1), and NSG mice were bred and maintained at the University of British Columbia Biomedical Research Centre. *Rag.Vav.G9a*$^{-/-}$ mice and *Rag.G9a*$^{fl/fl}$ mice were generated by crossing *Vav.G9a*$^{-/-}$ mice and control *G9a*$^{fl/fl}$ mice with *Rag1*$^{-/-}$ mice. All experiments were performed using sex-matched littermates. All mice were maintained in a specific pathogen–free environment. All experiments were performed at the University of British Columbia according to institutional and Canadian Council on Animal Care guidelines approved by the University of British Columbia Committee on Animal Care.

Cytokine administration. *G9a*$^{fl/fl}$ and *Vav.G9a*$^{-/-}$ mice were given intraperitoneal injections of 500 ng IL-33 (eBioscience) on days 0, 1, 2, and 3 as previously described (Price et al., 2010). Mice were euthanized 24 h after the final injection, and BM was harvested and analyzed.

BM chimeras. CD45.1 recipient mice were lethally irradiated with 10 Gy with an X-Rad (Precision X-Ray) and were reconstituted by intravenous injection of BM from CD45.1/2 mice mixed with either *G9a*$^{fl/fl}$ or *Vav.G9a*$^{-/-}$ BM cells (2.5×10^6 cells) to achieve an ~50:50 chimera after stable reconstitution. At least 8 wk after transplant, mice were euthanized, and BM and spleens were collected for analysis.

Lung inflammation models. For the short course of papain, *G9a*$^{fl/fl}$ and *Vav.G9a*$^{-/-}$ mice were anesthetized, followed by intranasal instillation of 10 µg papain in 40 µl PBS on days 0, 1, and 2. Mice were sacrificed on day 3, and BAL fluid and lungs were collected and analyzed. Intracellular cytokines

were detected after 4 h of stimulation with cell stimulation cocktail (plus protein transport inhibitors; eBioscience) using an intracellular fixation and permeabilization buffer set (eBioscience) according to the manufacturer's protocol with the antibodies IL-13 (eBio13A) and IL-17A (eBio17B7). Live cells were identified using fixable viability dye (eFluor 506; eBioscience). For the long course of papain, *G9a*$^{fl/fl}$ and *Vav.G9a*$^{-/-}$ mice were anesthetized and then sensitized with papain (10 µg in 40 µl) by intranasal instillation on days 0, 3, and 6. Mice were rechallenged on day 14, and BAL fluid and lungs were collected on day 15. HDM (*Dermatophagoides pteronyssinus*)-mediated allergic inflammation was induced in *G9a*$^{fl/fl}$ and *Vav.G9a*$^{-/-}$ mice by intranasal instillation with 100 µg HDM antigen (Greer Laboratories) on days 0, 1, and 2 and 25 µg on days 13, 14, 15, 16, and 17. Mice were sacrificed 24 h after the final challenge. BAL cells were enumerated and differentiated by flow cytometry with antibodies to CD3e (145-2C11), CD11c (N418), CD45 (I3/2), B220 (RA3-6B2), Siglec-F (E50-2440), and Ly6B (7/4).

Histology. Lung lobes were fixed in 10% buffered formalin solution and embedded into paraffin blocks. 5-µm sections were stained with periodic acid-Schiff (PAS). Airways were assessed for PAS staining as an indication of mucus hyperproduction. PAS$^+$ cells in the airways in each lung section were quantified.

Cell culture. iILC2s (live CD45$^+$ Lin$^-$ cKit$^-$ Sca1$^+$ CD25$^+$ ST2$^+$) were sorted from the BM of naive *G9a*$^{fl/fl}$ and *Vav.G9a*$^{-/-}$ mice. Approximately 5,000 cells were cultured in 200 µl IMDM containing 10% FCS, penicillin-streptomycin, and 150 µM monothioglycerol with 50 ng/ml rIL-2, 10 ng/ml rIL-7, and 100 ng/ml rIL-25. Cells were split and diluted 1:2 with fresh cytokine-containing media on day 3 and every other day thereafter. When used, the G9a inhibitor UNC0638 was added to cytokine-containing media at 0.5 µM. Live cells were counted by trypan blue exclusion. Intracellular cytokines were detected after 4 h of stimulation with 50 ng/ml PMA and 750 µg/ml ionomycin in the presence of 10 µg/ml brefeldin A using an intracellular fixation and permeabilization buffer set (eBioscience) according to the manufacturer's protocol with the antibodies IL-5 (TRFK5) and IL-17F (eBio18F10). Live cells were identified using eFluor 506 fixable viability dye.

RNA sequencing. ILC2s were sorted from BM and expanded in IL-2, IL-7, and IL-25 for 10 d. Cells were harvested and total RNA was extracted using an RNeasy Mini kit according to manufacturer's instructions (QIAGEN). Approximately 500 ng RNA was prepared with an mRNA kit (Truseq Stranded; Illumina) and sequenced on a MiSeq paired-end run (75 × 75; v3; Illumina). Samples were aligned to the 10-mm transcript reference using TopHat2, and differential expression was assessed using Cufflinks. The heat map of ILC2 and ILC3 core genes expressed in *G9a*$^{fl/fl}$ and *Vav.G9a*$^{-/-}$ iILC2s were generated using the open source R and VisR platforms (Younesy et al., 2015). Data are available through NCBI BioProject database accession no. PRJNA313104.

Quantitative real-time PCR (RT-PCR). RNA was isolated from expanded BM ILC2s using an RNeasy Mini kit according to the manufacturer's instructions (QIAGEN). Lung tissue was homogenized using a TissueLyser (QIAGEN). RNA was extracted using TRIzol (Invitrogen) and reverse transcribed with a high-capacity cDNA synthesis kit (Thermo Fisher Scientific), and gene expression was analyzed by quantitative RT-PCR with SYBR green chemistry (KAPA Biosystems) on an RT-PCR system (7900 Fast; Applied Biosystems). The primers used were obtained from QIAGEN or synthesized de novo: *Il5* forward, 5′-GATGAGGCTTCCTGTCCCTACTC-3′ and reverse, 5′-TCGCCACACTTCTCTTTTTGG-3′; *Il13* forward, 5′-CCTGGCTCTTGCTTGCCTT-3′ and reverse, 5′-GGTCTTGTGTGATGTTGCTCA-3′; *Il17f* forward, 5′-TGCTACTGTTGATGTTGGGAC-3′ and reverse, 5′-AATGCCCTGGTTTTGGTTGAA-3′; *Rorc* forward, 5′-TCCACTACGGGGTTATCACCT-3′ and reverse, 5′-AGTAGGCCACATTACACTGCT-3′; and *Actb* forward, 5′-GGCTGTATTCCCCTCCATCG-3′ and reverse, 5′-CCAGTTGGTAACAATGCCATGT-3′.

ChIP. ILC2s were sorted from BM and expanded in IL-2, IL-7, and IL-25 for 14 d. ChIP for H3K9me2 and H3K9/14Ac was conducted as previously described (Dong et al., 2008) using 1 µg of antibody specific to H3K9me2 (ab1220; Abcam) or H3K9/14Ac (06-599; EMD Millipore). After washing, elution, and reversion of cross-links, the DNA was isolated and used in quantitative PCR reactions on an RT-PCR system (ABI 7900 Fast). Data are presented as the ratio of immunoprecipitated to input cycle threshold (C_T) values. The primers used for PCR analysis were: *Il5* promoter forward, 5′-AAGTCTAGCTACCGCCAATA-3′ and reverse, 5′-AGCAAAGGTGAGTTCAATCT-3′; *Il13* promoter forward, 5′-GGGCAGGTGAGTATCAGTCTA-3′ and reverse, 5′-GTCTATATCCCTCCCACTCGT-3′; *Il17f* promoter forward, 5′-GGGAATCAAAGGGGGACCCTAA-3′ and reverse, 5′-AAAGCAGAACCCACACGCAGAG-3′; *Gata3* promoter forward, 5′-CGTATATGATGAGTCTTCTCTGGGACTTG-3′ and reverse, 5′-AAATCTCAGAACACACACATTTCCAGG-3′; and *Rorc* promotor forward, 5′-ATTCCATGAGGGCTTGCCT-3′ and reverse, 5′-ACCTGTCATCAGCCTCCCATA-3′.

Preparation of cell suspension. BM cells were isolated by flushing femurs and tibias with a 26-G needle though a 70-µm strainer. Lungs were minced and digested in 200 U/ml collagenase IV (Sigma-Aldrich) for 45 min at 37°C and passed through a 70-µm cell strainer. RBCs were lysed, and leukocytes were enriched using a Percoll (Sigma-Aldrich) separation. mLNs and Peyer's patches were passed through a 70-µm cell strainer to form single-cell suspensions. Small

intestine lamina propria cells were isolated by digestion in 0.5 mg/ml collagenase/dispase for 30 min after removal of intestinal epithelial cells. Leukocytes were enriched using a standard Percoll separation method.

Antibodies and flow cytometry. Staining and antibody dilutions were prepared in PBS containing 2% FCS, 2 mM EDTA, and 0.05% sodium azide. Samples were first blocked in buffer containing 5 µg/ml anti-CD16/32 (2.4G2) and 2% rat serum to block nonspecific antibody binding. Viable cells were identified using the eFluor 506 fixable viability dye. The following antibodies were used to identify ILCs: pan-CD45 (I3/2), lineage markers (CD3e [145-2C11 and KT3], CD5 [53-7.3], CD4 [GK1.5; not used when staining for ILC3s], CD8 [53.67], CD11c [N418], CD11b [M1/70], CD19 [1D3], NK1.1 [PK136], Gr1 [RB6-8C5], and Ter119 [TER-119]), CD25 (PC61.5), CD127 (SB/199), Sca1 (D7), cKit (ACK2), ST2 (RMST2-2), CD90.2 (53-2.1), KLRG1 (2F1), ICOS (7E.17G9), GATA3 (TWAJ), and RORγt (B2D). Additional antibodies used include IL-17RB (MUNC33), CD45.1 (A20), and CD45.2 (104).

NSG adoptive transfers. NSG-recipient mice were injected intravenously with 5,000 FACS-purified BM iILC2s ($CD45^+$ Lin^- c-kit^{low} Sca-1^{high} $CD25^+$ $CD127^+$) from *Vav.G9a*$^{-/-}$ mice and control *G9a*$^{fl/fl}$. After 3–4 wk, small intestinal lamina propria cells and lung cells were isolated and evaluated for the presence of ILC2s and ILC3s.

Statistics. Results represent the mean ± SEM. Statistical significance was determined by Student's *t* test using Prism 5.0 (GraphPad Software). A p-value <0.05 was considered significant.

Online supplemental material. Table S1 is a list of core ILC2 and ILC3 genes (Robinette et al., 2015) compared with control and G9a-deficient iILC2s. Online supplemental material is available at http://www.jem.org/cgi/content/full/jem.20151646/DC1.

ACKNOWLEDGMENTS

We thank Ryan Vander Werff for his technical assistance performing the RNA-seq experiment; the Biomedical Research Centre animal care facility; Taka Murakami of the Biomedical Research Centre genotyping facility; Andy Johnson and Justin Wong of the University of British Columbia flow cytometry facility; Les Rollins, Rupinder Dhesi, and Michael Williams of the Biomedical Research Centre core staff; Ingrid Barta of the Biomedical Research Centre histology facility; and K. Jacobsen for critically reading the manuscript.

This work was supported by the Canadian Institutes of Health Research's (CIHR) Canadian Epigenetics, Environment and Health Research Consortium (grant 128090 to C. Zaph) and operating grants (MOP-84545 to K.M. McNagny and MSH-95368, MOP-89773, and MOP-106623 to C. Zaph) and an Australian National Health and Medical Research Council project grant (APP1004466 to C. Zaph). The development of the mouse strains used in this study was supported by funds from the Leon Judah Blackmore Foundation to F.M. Rossi. F. Antignano is the recipient of a CIHR/Canadian Association of Gastroenterology/Crohn's and Colitis Foundation of Canada postdoctoral fellowship. M.J. Oudhoff is a Banting Fellow and a Michael Smith Foundation for Health Research Fellow. K.M. McNagny is a Michael Smith Foundation for Health Research Senior Scholar. F.M. Rossi is a Distinguished Scholar in Residence of the Peter Wall Institute for Advanced Studies. C. Zaph is a Michael Smith Foundation for Health Research Career Investigator and a Veski Innovation Fellow.

The authors declare no competing financial interests.

Submitted: 16 October 2015
Accepted: 22 April 2016

REFERENCES

Antignano, F., K. Burrows, M.R. Hughes, J.M. Han, K.J. Kron, N.M. Penrod, M.J. Oudhoff, S.K. Wang, P.H. Min, M.J. Gold, et al. 2014. Methyltransferase G9A regulates T cell differentiation during murine intestinal inflammation. *J. Clin. Invest.* 124:1945–1955. http://dx.doi.org/10.1172/JCI69592

Califano, D., J.J. Cho, M.N. Uddin, K.J. Lorentsen, Q. Yang, A. Bhandoola, H. Li, and D. Avram. 2015. Transcription factor Bcl11b controls identity and function of mature type 2 innate lymphoid cells. *Immunity.* 43:354–368. http://dx.doi.org/10.1016/j.immuni.2015.07.005

Chen, J., H. Liu, J. Liu, J. Qi, B. Wei, J. Yang, H. Liang, Y. Chen, J. Chen, Y. Wu, et al. 2012. H3K9 methylation is a barrier during somatic cell reprogramming into iPSCs. *Nat. Genet.* 45:34–42. http://dx.doi.org/10.1038/ng.2491

Cherrier, M., S. Sawa, and G. Eberl. 2012. Notch, Id2, and RORγt sequentially orchestrate the fetal development of lymphoid tissue inducer cells. *J. Exp. Med.* 209:729–740. http://dx.doi.org/10.1084/jem.20111594

Constantinides, M.G., B.D. McDonald, P.A. Verhoef, and A. Bendelac. 2014. A committed precursor to innate lymphoid cells. *Nature.* 508:397–401. http://dx.doi.org/10.1038/nature13047

Dong, K.B., I.A. Maksakova, F. Mohn, D. Leung, R. Appanah, S. Lee, H.W. Yang, L.L. Lam, D.L. Mager, D. Schübeler, et al. 2008. DNA methylation in ES cells requires the lysine methyltransferase G9a but not its catalytic activity. *EMBO J.* 27:2691–2701. http://dx.doi.org/10.1038/emboj.2008.193

Duan, Z., A. Zarebski, D. Montoya-Durango, H.L. Grimes, and M. Horwitz. 2005. Gfi1 coordinates epigenetic repression of p21Cip/WAF1 by recruitment of histone lysine methyltransferase G9a and histone deacetylase 1. *Mol. Cell. Biol.* 25:10338–10351. http://dx.doi.org/10.1128/MCB.25.23.10338-10351.2005

Eberl, G., S. Marmon, M.J. Sunshine, P.D. Rennert, Y. Choi, and D.R. Littman. 2004. An essential function for the nuclear receptor RORγt in the generation of fetal lymphoid tissue inducer cells. *Nat. Immunol.* 5:64–73. http://dx.doi.org/10.1038/ni1022

Gold, M.J., F. Antignano, T.Y. Halim, J.A. Hirota, M.R. Blanchet, C. Zaph, F. Takei, and K.M. McNagny. 2014. Group 2 innate lymphoid cells facilitate sensitization to local, but not systemic, T_H2-inducing allergen exposures. *J. Allergy Clin. Immunol.* 133:1142–1148.e5. http://dx.doi.org/10.1016/j.jaci.2014.02.033

Halim, T.Y., R.H. Krauss, A.C. Sun, and F. Takei. 2012a. Lung natural helper cells are a critical source of Th2 cell-type cytokines in protease allergen-induced airway inflammation. *Immunity.* 36:451–463. http://dx.doi.org/10.1016/j.immuni.2011.12.020

Halim, T.Y., A. MacLaren, M.T. Romanish, M.J. Gold, K.M. McNagny, and F. Takei. 2012b. Retinoic-acid-receptor-related orphan nuclear receptor alpha is required for natural helper cell development and allergic inflammation. *Immunity.* 37:463–474. http://dx.doi.org/10.1016/j.immuni.2012.06.012

Halim, T.Y., C.A. Steer, L. Mathä, M.J. Gold, I. Martinez-Gonzalez, K.M. McNagny, A.N. McKenzie, and F. Takei. 2014. Group 2 innate lymphoid cells are critical for the initiation of adaptive T helper 2 cell-mediated allergic lung inflammation. *Immunity.* 40:425–435. http://dx.doi.org/10.1016/j.immuni.2014.01.011

Hoyler, T., C.S. Klose, A. Souabni, A. Turqueti-Neves, D. Pfeifer, E.L. Rawlins, D. Voehringer, M. Busslinger, and A. Diefenbach. 2012. The transcription factor GATA-3 controls cell fate and maintenance of type 2 innate lymphoid cells. *Immunity.* 37:634–648. http://dx.doi.org/10.1016/j.immuni.2012.06.020

Klose, C.S., M. Flach, L. Möhle, L. Rogell, T. Hoyler, K. Ebert, C. Fabiunke, D. Pfeifer, V. Sexl, D. Fonseca-Pereira, et al. 2014. Differentiation of type 1 ILCs from a common progenitor to all helper-like innate lymphoid cell lineages. *Cell.* 157:340–356. http://dx.doi.org/10.1016/j.cell.2014.03.030

Kurebayashi, S., E. Ueda, M. Sakaue, D.D. Patel, A. Medvedev, F. Zhang, and A.M. Jetten. 2000. Retinoid-related orphan receptor γ (RORγ) is essential for lymphoid organogenesis and controls apoptosis during thymopoiesis. *Proc. Natl. Acad. Sci. USA.* 97:10132–10137. http://dx.doi.org/10.1073/pnas.97.18.10132

Lehnertz, B., J.P. Northrop, F. Antignano, K. Burrows, S. Hadidi, S.C. Mullaly, F.M. Rossi, and C. Zaph. 2010. Activating and inhibitory functions for the histone lysine methyltransferase G9a in T helper cell differentiation and function. *J. Exp. Med.* 207:915–922. http://dx.doi.org/10.1084/jem.20100363

Moro, K., T. Yamada, M. Tanabe, T. Takeuchi, T. Ikawa, H. Kawamoto, J. Furusawa, M. Ohtani, H. Fujii, and S. Koyasu. 2010. Innate production of T_H2 cytokines by adipose tissue-associated c-Kit$^+$Sca-1$^+$ lymphoid cells. *Nature.* 463:540–544. http://dx.doi.org/10.1038/nature08636

Neill, D.R., S.H. Wong, A. Bellosi, R.J. Flynn, M. Daly, T.K. Langford, C. Bucks, C.M. Kane, P.G. Fallon, R. Pannell, et al. 2010. Nuocytes represent a new innate effector leukocyte that mediates type-2 immunity. *Nature.* 464:1367–1370. http://dx.doi.org/10.1038/nature08900

Oboki, K., T. Ohno, N. Kajiwara, K. Arae, H. Morita, A. Ishii, A. Nambu, T. Abe, H. Kiyonari, K. Matsumoto, et al. 2010. IL-33 is a crucial amplifier of innate rather than acquired immunity. *Proc. Natl. Acad. Sci. USA.* 107:18581–18586. http://dx.doi.org/10.1073/pnas.1003059107

Possot, C., S. Schmutz, S. Chea, L. Boucontet, A. Louise, A. Cumano, and R. Golub. 2011. Notch signaling is necessary for adult, but not fetal, development of RORγt$^+$ innate lymphoid cells. *Nat. Immunol.* 12:949–958. http://dx.doi.org/10.1038/ni.2105

Price, A.E., H.E. Liang, B.M. Sullivan, R.L. Reinhardt, C.J. Eisley, D.J. Erle, and R.M. Locksley. 2010. Systemically dispersed innate IL-13–expressing cells in type 2 immunity. *Proc. Natl. Acad. Sci. USA.* 107:11489–11494. http://dx.doi.org/10.1073/pnas.1003988107

Robinette, M.L., A. Fuchs, V.S. Cortez, J.S. Lee, Y. Wang, S.K. Durum, S. Gilfillan, and M. Colonna. Immunological Genome Consortium. 2015. Transcriptional programs define molecular characteristics of innate lymphoid cell classes and subsets. *Nat. Immunol.* 16:306–317. http://dx.doi.org/10.1038/ni.3094

Sanos, S.L., V.L. Bui, A. Mortha, K. Oberle, C. Heners, C. Johner, and A. Diefenbach. 2009. RORγt and commensal microflora are required for the differentiation of mucosal interleukin 22-producing NKp46$^+$ cells. *Nat. Immunol.* 10:83–91. http://dx.doi.org/10.1038/ni.1684

Satoh-Takayama, N., S. Lesjean-Pottier, P. Vieira, S. Sawa, G. Eberl, C.A. Vosshenrich, and J.P. Di Santo. 2010. IL-7 and IL-15 independently program the differentiation of intestinal CD3$^-$NKp46$^+$ cell subsets from Id2-dependent precursors. *J. Exp. Med.* 207:273–280. http://dx.doi.org/10.1084/jem.20092029

Serafini, N., R.G. Klein Wolterink, N. Satoh-Takayama, W. Xu, C.A. Vosshenrich, R.W. Hendriks, and J.P. Di Santo. 2014. Gata3 drives development of RORγt$^+$ group 3 innate lymphoid cells. *J. Exp. Med.* 211:199–208. http://dx.doi.org/10.1084/jem.20131038

Spooner, C.J., J. Lesch, D. Yan, A.A. Khan, A. Abbas, V. Ramirez-Carrozzi, M. Zhou, R. Soriano, J. Eastham-Anderson, L. Diehl, et al. 2013. Specification of type 2 innate lymphocytes by the transcriptional determinant Gfi1. *Nat. Immunol.* 14:1229–1236. http://dx.doi.org/10.1038/ni.2743

Sun, Z., D. Unutmaz, Y.R. Zou, M.J. Sunshine, A. Pierani, S. Brenner-Morton, R.E. Mebius, and D.R. Littman. 2000. Requirement for RORγ in thymocyte survival and lymphoid organ development. *Science.* 288:2369–2373. http://dx.doi.org/10.1126/science.288.5475.2369

Tachibana, M., K. Sugimoto, M. Nozaki, J. Ueda, T. Ohta, M. Ohki, M. Fukuda, N. Takeda, H. Niida, H. Kato, and Y. Shinkai. 2002. G9a histone methyltransferase plays a dominant role in euchromatic histone H3 lysine 9 methylation and is essential for early embryogenesis. *Genes Dev.* 16:1779–1791. http://dx.doi.org/10.1101/gad.989402

Vedadi, M., D. Barsyte-Lovejoy, F. Liu, S. Rival-Gervier, A. Allali-Hassani, V. Labrie, T.J. Wigle, P.A. Dimaggio, G.A. Wasney, A. Siarheyeva, et al. 2011. A chemical probe selectively inhibits G9a and GLP methyltransferase activity in cells. *Nat. Chem. Biol.* 7:566–574. http://dx.doi.org/10.1038/nchembio.599

Wen, B., H. Wu, Y. Shinkai, R.A. Irizarry, and A.P. Feinberg. 2009. Large histone H3 lysine 9 dimethylated chromatin blocks distinguish differentiated from embryonic stem cells. *Nat. Genet.* 41:246–250. http://dx.doi.org/10.1038/ng.297

Wong, S.H., J.A. Walker, H.E. Jolin, L.F. Drynan, E. Hams, A. Camelo, J.L. Barlow, D.R. Neill, V. Panova, U. Koch, et al. 2012. Transcription factor RORα is critical for nuocyte development. *Nat. Immunol.* 13:229–236. http://dx.doi.org/10.1038/ni.2208

Yagi, R., C. Zhong, D.L. Northrup, F. Yu, N. Bouladoux, S. Spencer, G. Hu, L. Barron, S. Sharma, T. Nakayama, et al. 2014. The transcription factor GATA3 is critical for the development of all IL-7Rα-expressing innate lymphoid cells. *Immunity.* 40:378–388. http://dx.doi.org/10.1016/j.immuni.2014.01.012

Yang, Q., L.A. Monticelli, S.A. Saenz, A.W. Chi, G.F. Sonnenberg, J. Tang, M.E. De Obaldia, W. Bailis, J.L. Bryson, K. Toscano, et al. 2013. T cell factor 1 is required for group 2 innate lymphoid cell generation. *Immunity.* 38:694–704. http://dx.doi.org/10.1016/j.immuni.2012.12.003

Younesy, H., T. Möller, M.C. Lorincz, M.M. Karimi, and S.J. Jones. 2015. VisRseq: R-based visual framework for analysis of sequencing data. *BMC Bioinformatics.* 16:S2. http://dx.doi.org/10.1186/1471-2105-16-S11-S2